Selected Paper

Doppler-Free Two-Photon Excitation Spectroscopy and the Zeeman Effect in the "Channel Three" Region of C_6H_6

Dae Youl Baek,[1] JinHai Chen,[1] Jinguo Wang,[1] Atsushi Doi,[1] Shunji Kasahara,[1] Masaaki Baba,[2] and Hajime Katô*[1]

[1]Molecular Photoscience Research Center, Kobe University, Nada-ku, Kobe 657-8501

[2]Department of Chemistry, Graduate School of Science, Kyoto University, Kyoto 606-8502

Received July 13, 2005; E-mail: h-kato@kobe-u.ac.jp

Doppler-free two-photon excitation spectra and the Zeeman effects for the $1_0^2 14_0^1$ and $1_0^1 14_0^1$ bands, whose vibrational excess energies are 3412 and 2492 cm^{-1}, respectively, of the $S_1\ ^1B_{2u} \leftarrow S_0\ ^1A_{1g}$ transition in gaseous benzene-h_6 have been measured. Rotationally resolved lines up to a rotational excess energy of 945 cm^{-1} in the $1_0^1 14_0^1$ band, whose excess energy is isoenergetic with the one of the $1_0^2 14_0^1$ band at low J, have been observed. The density of perturbation is observed to increase around the $K = 0$ and $K = J$ levels in the $1_0^1 14_0^1$ band as the rotational energy increases, but line broadening is not observed. It was reported that only the $K = 0$ lines at low J and the $K = J$ lines at high J were observed as a sharp line and the rest was washed out by broadening in the $1_0^2 14_0^1$ band. The assignments are confirmed by the Zeeman spectra. The character and magnitude of Zeeman splittings in both bands could be understood as originating from the electronic orbital angular momentum arising from a mixing of the $S_1\ ^1B_{2u}$ and $S_2\ ^1B_{1u}$ states via J–L coupling. The levels of the $S_1\ ^1B_{2u}$ state are found not to be mixed with a triplet state by the Zeeman effect.

Benzene is a prototype aromatic molecule, and its dynamics in excited states have been studied extensively.[1–5] Terminologies for radiationless transitions are *intersystem crossing* (ISC) and *internal conversion* (IC) in the time dependent picture, and *intersystem mixing* and *internal mixing* in the stationary state picture.[1] The fluorescence quantum yield of the $S_1\ ^1B_{2u}$ state of an isolated benzene was observed to be small, and the nonradiative decays excited to low vibrational levels of the S_1 state were attributed to ISC: nonradiative transition to isoenergetic levels of vibrationally highly excited levels of the triplet state $T_1\ ^3B_{1u}$.[6–13] Callomon et al.[14] observed that the rotational structure of the $S_1 \leftarrow S_0$ transition became partly or wholly washed out for excess energies higher than 3000 cm^{-1}. Because it was thought that fluorescence and ISC could not account for this phenomenon, the term "channel three" was introduced to describe the nonradiative process. Doppler-free high resolution spectra of benzene were measured extensively by Neusser et al.[15–32] Compared to the $1_0^1 14_0^1$ band ($E_{excess} = 2492\ cm^{-1}$), a drastically reduced number of sharp lines were observed in the $1_0^2 14_0^1$ band ($E_{excess} = 3412\ cm^{-1}$).[18,19,22] At the blue edge of the $1_0^2 14_0^1$ band, where lines of low J were expected, only rotational lines with $K = 0$ were observed, while many other lines with $K \neq 0$ disappeared. J and K are the quantum numbers of rotational angular momentum and its projection along the c axis, respectively. At the red part starting 3.3 cm^{-1} away from the band origin, where lines of high J existed, rotational lines with $K = J$ were observed to be dominant. The spectrum in the blue part was explained by line broadening due to a shortening of the lifetime induced by a parallel Coriolis interaction, and the spectrum in the red part was explained by one induced by a perpendicular Coriolis interaction. Riedle et al.[32] measured the rotationally resolved fluorescence excitation and resonance enhanced multiphoton ionization spectra of the $1_0^3 6_0^1$ band at the onset of channel three, and the optically excited rovibronic states were thought to be coupled to background states within S_1, which are themselves broadened due to strong coupling to the highly excited S_0 state. Helman and Marcus[33,34] proposed a theoretical treatment of fluorescence excitation spectra. A quasistationary molecular eigenstate in the S_1 state is first calculated by taking account of the vibration–rotation coupling to the zeroth-order states. The S_1 eigenstate is then coupled via the nonadiabatic nuclear kinetic operator to rovibronic states in the S_0 state. The calculated results applied to the $1_0^2 14_0^1$ band were in very good agreement with the experimental findings, and it was demonstrated that the onset of channel three occurs via anharmonic-Coriolis coupling in the S_1 state plus IC to the S_0 state.

Recently, we have measured the rotationally resolved spectra and the Zeeman effects of the 6_0^1, $1_0^1 6_0^1$, $1_0^2 6_0^1$, and $1_0^1 14_0^1$ bands of the $S_1 \leftarrow S_0$ transition of C_6H_6 and the 14_0^1 and $1_0^1 14_0^1$ bands of the $S_1 \leftarrow S_0$ transition of C_6D_6.[35–38] From the analysis, the Zeeman splitting has been shown to originate from the electronic orbital angular momentum arising from a mixing of the $S_1\ ^1B_{2u}$ and $S_2\ ^1B_{1u}$ states via J–L coupling, and it has been demonstrated that all of the rotationally resolved levels are not mixed with a triplet state. Accordingly, it was concluded that intersystem mixing does not occur at levels of low excess energy in the S_1 state of isolated benzene, and nonradiative decay occurs through internal mixing followed by rotational and vibrational relaxation in the S_0 state.

Riedle et al.[31] studied the $1_0^2 14_0^1 16_2^2$ band of C_6H_6 and the $1_0^2 14_0^2$ band of $^{13}C_6H_6$, and the decay behavior was reported to depend strongly on the excess energy and the rotational quantum numbers rather than on the vibrational character

Published on the web January 13, 2006; DOI 10.1246/bcsj.79.75

and symmetry of the excited state.[31] We have extended measurements of Doppler-free two-photon excitation (DFTPE) spectra and the Zeeman effects of the $1_0^1 14_0^1$ band up to high J and K levels, which are isoenergetic with levels of the $1_0^2 14_0^1$ band at low J. The Zeeman spectrum of the $1_0^2 14_0^1$ band has also been measured. The results and analysis are reported in this paper.

Results and Discussion

The experimental setup for DFTPE spectroscopy was similar to that reported in Ref. 35. DFTPE spectra of the $1_0^1 14_0^1$ band of the $S_1 \leftarrow S_0$ transition of gaseous benzene-h_6 (1 Torr) were measured in the range of 40532.7 to 40578.3 cm^{-1} at magnetic fields of $H = 0$ and 1.2 T. In total, 2373 lines of $^{Q(K)}Q(J)$ transitions were assigned, and the data field is shown in Fig. 1. By fixing the molecular constants of the $S_0\ ^1A_{1g}$ ($v = 0$) state to those reported in Ref. 39, the molecular constants of the $S_1\ ^1B_{2u}$ ($v_1 = 1$, $v_{14} = 1$) state were determined by a least-squares fitting to all of the assigned lines. The results are listed in Table 1.

In our previous studies,[35] the Zeeman splittings of the $^{Q(K)}Q(J)$ lines were reported to increase as K increases for a given J. In the present study, we have plotted the magnitude of the Zeeman splitting of the $^{Q(K)}Q(J)$ line of a given J against K, and it has become clear that the magnitude increases in proportion to K^2 (see Fig. 2). The Zeeman splittings of the $^{Q(K=J)}Q(J)$ lines were observed to increase in proportion to J (see Fig. 7 in Ref. 35). The same phenomenon was also found for the 14_0^1 band of benzene-d_6,[37] and it was shown that the $S_1\ ^1B_{2u}$ state mixes with the $S_2\ ^1B_{1u}$ state via J–L coupling. The Zeeman splitting of the $^{Q(K)}Q(J)$ line is given by

$$\frac{8CK^2}{J+1}\frac{|\langle S_2\ ^1B_{1u}|L_z|S_1\ ^1B_{2u}\rangle|^2}{E(S_2)-E(S_1)}\mu_B H, \quad (1)$$

where C is the rotational constant along the c axis, L_z is the electronic orbital angular momentum along the molecule fixed z axis (c axis), and μ_B is the Bohr magneton. The matrix element $\langle S_2\ ^1B_{1u}|L_z|S_1\ ^1B_{2u}\rangle$ was evaluated to be -1.729 in units of $\hbar$ from simple molecular orbitals.[36] By using this value, $C = 0.0906\ cm^{-1}$, $E(S_1) = 38086\ cm^{-1}$, and $E(S_2) = 46500\ cm^{-1}$ (the later two were taken from Refs. 40 and 41), the Zeeman splitting of the $S_1\ ^1B_{2u}$ ($v_1 = 1$, $v_{14} = 1$, $J = 55$, $K = 55$) level at $H = 1.2$ T was calculated by Eq. 1 to be $0.0078\ cm^{-1}$. The observed value was $0.0106\ cm^{-1}$. Thus, the Zeeman splitting

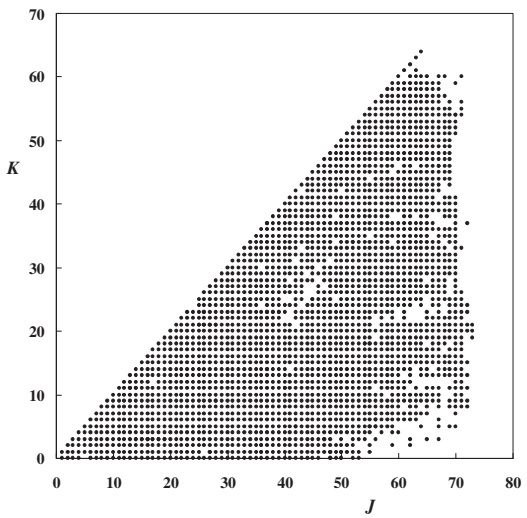

Fig. 1. Data field of the $1_0^1 14_0^1$ band of the $S_1\ ^1B_{2u} \leftarrow S_0\ ^1A_{1g}$ transition of benzene-h_6.

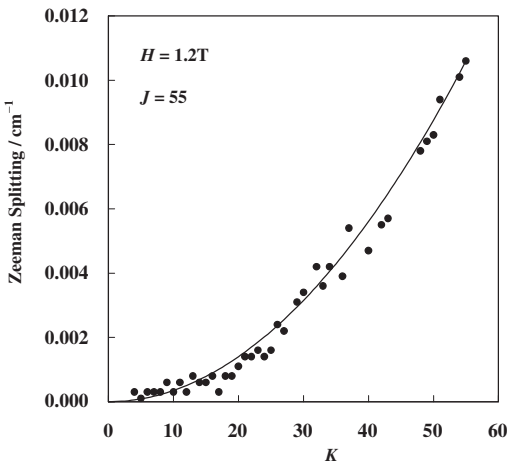

Fig. 2. The K dependence of the observed Zeeman splittings of the $^{Q(K)}Q(J = 55)$ lines of the $1_0^1 14_0^1$ band. The Zeeman splitting of the $^{Q(55)}Q(55)$ line was 0.0106 cm^{-1}, and the solid line is a function $0.0106K^2/55^2$ in units of cm^{-1}.

Table 1. Molecular Constants of the $S_1\ ^1B_{2u}$ ($v_1 = 1$, $v_{14} = 1$) and $S_1\ ^1B_{2u}$ ($v_1 = 2$, $v_{14} = 1$) States of Benzene-h_6 in Units of cm^{-1}

	$S_1\ ^1B_{2u}$ ($v_1 = 1$, $v_{14} = 1$) This work	$S_1\ ^1B_{2u}$ ($v_1 = 2$, $v_{14} = 1$) This work	$S_0\ ^1A_{1g}$ ($v = 0$) Ref. 39
$B\ (= A)$	0.1811561(7)	0.1810582(19)[b]	0.1897717(3)
C	0.0905979(11)	0.090764(32)[c]	0.09488585(15)
D_J ($\times 10^7$)	0.460(14)		0.408(4)
D_{JK} ($\times 10^7$)	−0.862(4)		−0.660(11)
D_K ($\times 10^7$)	0.193(3)	1.27(25)[c]	
v_0	40578.2743(6)	41498.4604(3)[b]	
χ[a]	0.011	0.0008[b] 0.0348[c]	
N[a]	2373	18[b] 19[c]	

a) χ is the standard deviation and N is the number of data used for the fitting. b) Fitted for levels of $K = 0$. c) Fitted for levels of $K = J$ by fixing B and v_0.

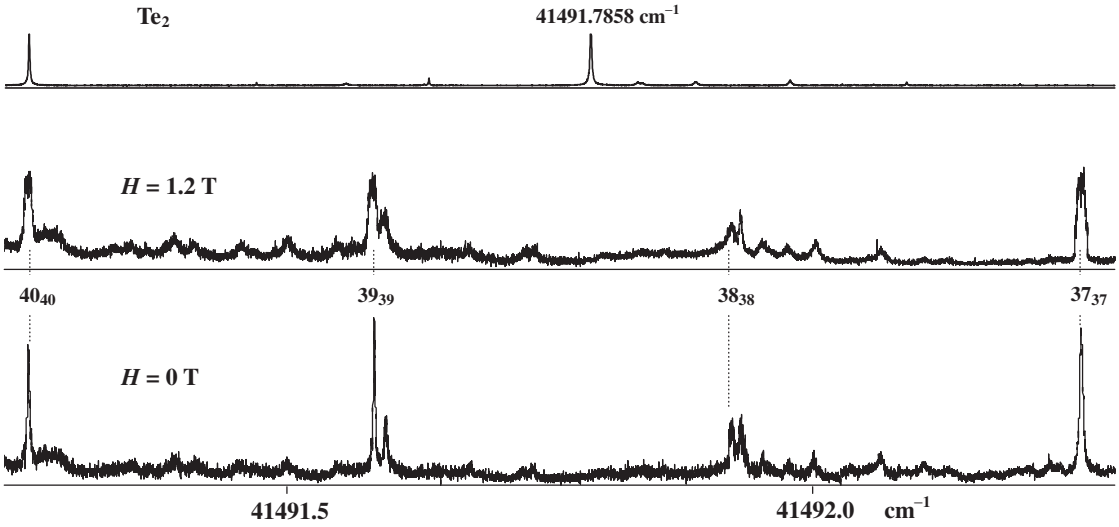

Fig. 3. DFTPE and Zeeman spectra at the red part 7.0 cm^{-1} away from the band origin. Assignments of the $^{Q(K)}Q(J)$ lines are indicated as J_K. The first trace is a Doppler-free absorption spectrum of the Te_2 molecule, which is used to calibrate the absolute wavenumber.

of the $^{Q(K)}Q(J)$ line expressed by Eq. 1 is consistent with the observations that (i) Zeeman splittings of the $^{Q(K)}Q(J)$ lines of a given J increase in proportion to K^2, (ii) Zeeman splittings of the $^{Q(K=J)}Q(J)$ lines increase in proportion to J at a large J, and (iii) the magnitude of the Zeeman splitting evaluated by Eq. 1 is in good agreement with the observed value. Accordingly, the observed Zeeman splittings originate from the electronic orbital angular momentum arising from a mixing of the $S_1\ ^1B_{2u}$ state with the $S_2\ ^1B_{1u}$ state via J–L coupling. The origin of the Zeeman splitting discussed in Ref. 35 must be corrected.

The transition energy of the $^{Q(8)}Q(72)$ line, which lies near the lower limit of the present observation, is 40533.0842 cm^{-1}. The rotational energy of the excited level is 945 cm^{-1}, and the vibrational–rotational excess energy of the level is 3437 cm^{-1}, which is higher than the excess energy of the $1_0^2 14_0^1$ band at low J. In the region of lines of high excess energy, the density of perturbation is observed to be high, and the assignment of many lines becomes difficult. However, broadening of the spectral line is not observed. This demonstrates that line broadening depends not only on excess energy, but also on the vibrational character of the excited state.

DFTPE spectra of the $1_0^2 14_0^1$ band of the $S_1 \leftarrow S_0$ transition of gaseous benzene-h_6 (1 Torr) were measured in the range of 41491.3 to 41498.5 cm^{-1} at magnetic fields of $H = 0$ and 1.2 T. Zeeman spectra have been found to be very useful also to assign the spectral lines[35–38] by the characters; (i) Zeeman splittings of the $^{Q(K)}Q(J)$ lines of a given J increase in proportion to K^2, (ii) Zeeman splittings of the $^{Q(K=J)}Q(J)$ lines increase in proportion to J. No appreciable Zeeman splitting was observed for the lines at the blue edge of the $1_0^2 14_0^1$ band, and therefore the previous assignments,[18,19,22] where only rotational lines with $K = 0$ were observed while many other lines with $K \neq 0$ disappeared, were confirmed. DFTPE and Zeeman spectra at the red part 7.0 cm^{-1} away from the band origin are shown in Fig. 3. Significant Zeeman splitting was observed for lines assigned as $^{Q(37)}Q(37) - {}^{Q(40)}Q(40)$, whose DFTPE spectra were observed to be sharp. Therefore, the previous assignments,[18,19,22] where rotational lines with $K = J$ were observed to be dominant in the region of high J, were confirmed. DFTPE and Zeeman spectra in the region of 41495.8–41496.7 cm^{-1} are shown in Fig. 4. The line width of the $K = 0$ lines changes appreciably from sharp to broad for $J = 14$–17, although the Zeeman splittings are not significant. On the other hand, the Zeeman splittings are significant for lines assigned as $^{Q(20)}Q(20) - {}^{Q(24)}Q(24)$.

Since the positions of the $^{Q(K=J)}Q(J)$ lines were found to be irregular, molecular constants B ($= A$) and ν_0 of the $S_1\ ^1B_{2u}$ ($\nu_1 = 2$, $\nu_{14} = 1$) state were determined by a least-squares fitting for transition energies of $^{Q(0)}Q(J)$ lines by fixing the molecular constants of the $S_0\ ^1A_{1g}$ ($\nu = 0$) state to those reported in Ref. 39. Then, by fixing the B and ν_0, the molecular constants C and D_K were determined by a least-squares fitting for transition energies of $^{Q(K=J)}Q(J)$ lines. The resulting molecular constants are listed in Table 1. The difference between the observed transition energy E_{obs} and the energy E_{cal} calculated from the molecular constants is plotted in Fig. 5 for all of the assigned lines. The agreement is good for $^{Q(0)}Q(J)$ lines, but poor for $^{Q(K=J)}Q(J)$ lines. This is reasonable because the matrix element of the parallel Coriolis interaction is proportional to K with the selection rule $\Delta K = 0$ and the matrix element of the perpendicular Coriolis interaction is proportional to $[J(J+1) - K(K \pm 1)]^{1/2}$ with the selection rule $\Delta K = \pm 1$: The parallel Coriolis interaction for a level of $K = 0$ is zero, but the perpendicular Coriolis interaction for a level of $K = J$ is not zero. These results support the previous conclusion,[32–34] that the spectrum in the blue part is due to line broadening induced through parallel Coriolis interaction and the spectrum in the red part is due to line broadening induced through perpendicular Coriolis interaction. Unassigned lines may be mostly transitions to levels of K close to J.

The J dependence of the Zeeman splitting for $^{Q(K=J)}Q(J)$ lines of the $1_0^2 14_0^1$ band at $H = 1.2$ T is shown in Fig. 6. The Zeeman splitting of the $K = J$ lines increases in proportion to J as it was observed in the $1_0^1 14_0^1$ band. The Zeeman

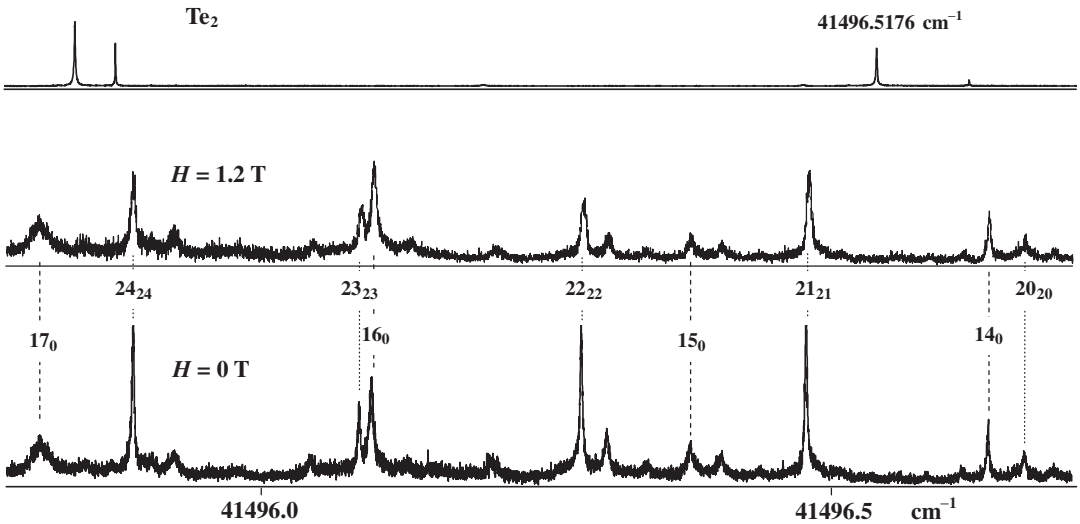

Fig. 4. DFTPE and Zeeman spectra in the region of 41495.8–41496.7 cm^{-1}. Assignments of the $^{Q(K)}Q(J)$ lines are indicated as J_K. The first trace is a Doppler-free absorption spectrum of the Te_2 molecule, which is used to calibrate the absolute wavenumber.

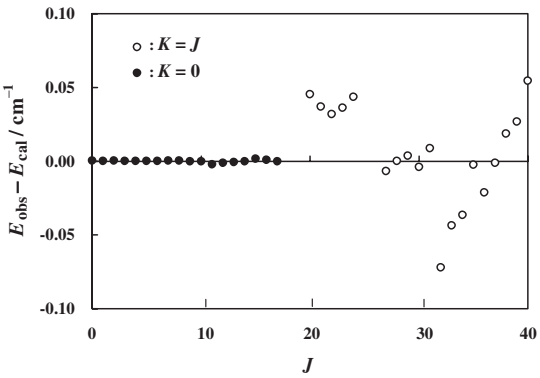

Fig. 5. The difference between the observed transition energy E_{obs} and the energy E_{cal} calculated from the molecular constants is plotted by a bullet (●) for the $^{Q(0)}Q(J)$ line and by an open circle (○) for the $^{Q(K=J)}Q(J)$ line.

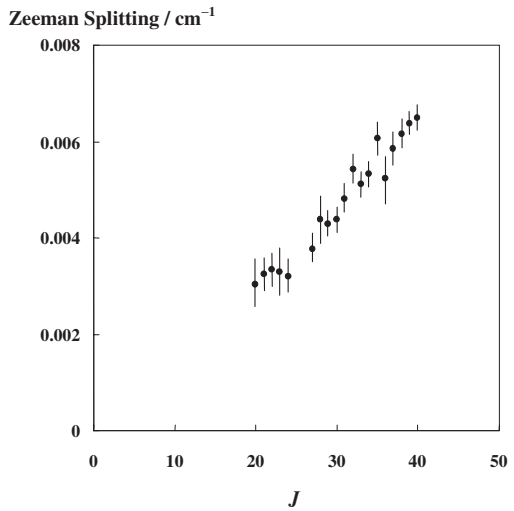

Fig. 6. J dependence of the observed Zeeman splittings of the $^{Q(K=J)}Q(J)$ line at $H = 1.2$ T.

splitting of the $^{Q(K=J)}Q(J)$ line of the $1_0^2 14_0^1$ band is slightly larger than the one of the $1_0^1 14_0^1$ band: The Zeeman splitting of the $^{Q(40)}Q(40)$ line at $H = 1.2$ T is 0.0065 cm^{-1} in the $1_0^2 14_0^1$ band and 0.0054 cm^{-1} in the $1_0^1 14_0^1$ band (see Fig. 6 in this work and Fig. 7 in Ref. 35). The fact that the Zeeman splittings of $^{Q(K=J)}Q(J)$ lines from the same J and K level in the S_0 $^1A_{1g}$ ($\nu = 0$) state are different in the $1_0^2 14_0^1$ and $1_0^1 14_0^1$ bands is consistent with the discovery that the observed Zeeman splitting originates from one of the upper state S_1 $^1B_{2u}$.

Conclusion

Rotationally resolved lines up to the rotational excess energy 945 cm^{-1} in the $1_0^1 14_0^1$ band, whose excess energy is isoenergetic with the one of the $1_0^2 14_0^1$ band at low J, were observed. The density of perturbation was observed to increase around the $K = 0$ and $K = J$ levels in the $1_0^1 14_0^1$ band as the rotational energy increases, but line broadening was not observed. This demonstrates that the line broadening depends not only on excess energy, but also on the vibrational character of the excited state. The IC to isoenergetic levels of vibrationally highly excited levels of the S_0 state depends on the vibrational character and symmetry of an excited level of the S_1 state.

Zeeman splittings observed in the $1_0^1 14_0^1$ and $1_0^2 14_0^1$ bands of the $S_1 \leftarrow S_0$ transition could be explained as those originate from the electronic orbital angular momentum arising from a mixing of the S_1 $^1B_{2u}$ and S_2 $^1B_{1u}$ states via J–L coupling. Mixing of a triplet state to the S_1 $^1B_{2u}$ state is excluded from the character and the magnitude of the observed Zeeman splittings as it was shown in Ref. 37. Accordingly, intersystem mixing does not occur in the region of the $1_0^1 14_0^1$ and $1_0^2 14_0^1$ bands of the S_1 state of isolated benzene.

The present results on the $1_0^2 14_0^1$ band support the previous conclusion that the spectrum in the blue part can be explained by a shortening of the lifetime (line broadening) due to IC to the S_0 state induced through parallel Coriolis interaction in the S_1 state, and that the spectrum in the red part can be

explained by the one induced through perpendicular Coriolis interaction in the S_1 state. The nonradiative decay of the S_1 $^1B_{2u}$ ($\nu_1 = 1$, $\nu_{14} = 1$) level occurs also through internal mixing to vibrationally highly excited levels of the S_0 state, which is enhanced by anharmonic-Coriolis coupling within the S_1 state, followed by rotational and vibrational relaxation in the S_0 state.

References

1 B. R. Henry, M. Kasha, *Annu. Rev. Phys. Chem.* **1968**, *19*, 161.
2 C. S. Parmenter, *Adv. Chem. Phys.* **1972**, *22*, 365.
3 P. Avouris, W. M. Gelbart, M. A. El-Sayed, *Chem. Rev.* **1977**, *77*, 793.
4 L. D. Ziegler, B. S. Hudson, *Excited States* **1982**, *5*, 41.
5 E. C. Lim, *Adv. Photochem.* **1997**, *23*, 165.
6 B. K. Selinger, W. R. Ware, *J. Chem. Phys.* **1970**, *53*, 3160.
7 C. S. Parmenter, M. W. Schuyler, *Chem. Phys. Lett.* **1970**, *6*, 339.
8 W. R. Ware, B. K. Selinger, C. S. Parmenter, M. W. Schuyler, *Chem. Phys. Lett.* **1970**, *6*, 342.
9 W. M. Gelbart, K. G. Spears, K. F. Freed, J. Jortner, S. A. Rice, *Chem. Phys. Lett.* **1970**, *6*, 345.
10 K. G. Spears, S. A. Rice, *J. Chem. Phys.* **1971**, *55*, 5561.
11 A. S. Abramson, K. G. Spears, S. A. Rice, *J. Chem. Phys.* **1972**, *56*, 2291.
12 M. A. Duncan, T. G. Dietz, M. G. Liverman, R. E. Smalley, *J. Phys. Chem.* **1981**, *85*, 7.
13 C. E. Otis, J. L. Knee, P. M. Johnson, *J. Chem. Phys.* **1983**, *78*, 2091.
14 J. H. Callomon, J. E. Parkin, R. Lopez-Delgado, *Chem. Phys. Lett.* **1972**, *13*, 125.
15 L. Wunsch, F. Metz, H. J. Neusser, E. W. Schlag, *J. Chem. Phys.* **1977**, *66*, 386.
16 E. Riedle, H. J. Neusser, E. W. Schlag, *J. Chem. Phys.* **1981**, *75*, 4231.
17 E. Riedle, R. Moder, H. J. Neusser, *Opt. Commun.* **1982**, *43*, 388.
18 E. Riedle, H. J. Neusser, E. W. Schlag, *J. Phys. Chem.* **1982**, *86*, 4847.
19 E. Riedle, H. J. Neusser, E. W. Schlag, *Faraday Discuss. Chem. Soc.* **1983**, *75*, 387.
20 E. Riedle, H. J. Neusser, E. W. Schlag, S. H. Lin, *J. Phys. Chem.* **1984**, *88*, 198.
21 E. Riedle, H. Stepp, H. J. Neusser, *Chem. Phys. Lett.* **1984**, *110*, 452.
22 E. Riedle, H. J. Neusser, *J. Chem. Phys.* **1984**, *80*, 4686.
23 U. Schubert, E. Riedle, H. J. Neusser, *J. Chem. Phys.* **1986**, *84*, 5326.
24 H. J. Neusser, E. Riedle, *Comments At. Mol. Phys.* **1987**, *19*, 331.
25 H. Sieber, E. Riedle, H. J. Neusser, *J. Chem. Phys.* **1988**, *89*, 4620.
26 H. J. Neusser, U. Schubert, E. Riedle, A. Kiermeier, H. Kühlewind, E. W. Schlag, *Ber. Bunsen-Ges. Phys. Chem.* **1988**, *92*, 322.
27 U. Schubert, E. Riedle, H. J. Neusser, *J. Chem. Phys.* **1989**, *90*, 5994.
28 E. Riedle, T. Knittel, T. Weber, H. J. Neusser, *J. Chem. Phys.* **1989**, *91*, 4555.
29 U. Schubert, E. Riedle, H. J. Neusser, E. W. Schlag, *Isr. J. Chem.* **1990**, *30*, 197.
30 T. Weber, E. Riedle, H. J. Neusser, *J. Opt. Soc. Am. B* **1990**, *7*, 1875.
31 E. Riedle, H. J. Neusser, E. W. Schlag, *Philos. Trans. R. Soc. London, Ser. A* **1990**, *332*, 189.
32 E. Riedle, T. Weber, U. Schubert, H. J. Neusser, E. W. Schlag, *J. Chem. Phys.* **1990**, *93*, 967.
33 A. Helman, R. A. Marcus, *J. Chem. Phys.* **1993**, *99*, 5002.
34 A. Helman, R. A. Marcus, *J. Chem. Phys.* **1993**, *99*, 5011.
35 M. Misono, J. Wang, M. Ushino, M. Okubo, H. Katô, M. Baba, S. Nagakura, *J. Chem. Phys.* **2002**, *116*, 162.
36 A. Doi, S. Kasahara, H. Katô, M. Baba, *J. Chem. Phys.* **2004**, *120*, 6439.
37 J. Wang, A. Doi, S. Kasahara, H. Katô, M. Baba, *J. Chem. Phys.* **2004**, *121*, 9188.
38 D. Y. Baek, J. Wang, A. Doi, S. Kasahara, H. Katô, M. Baba, *J. Phys. Chem. A* **2005**, *109*, 7127.
39 A. Doi, M. Baba, S. Kasahara, H. Katô, *J. Mol. Spectrosc.* **2004**, *227*, 180.
40 J. H. Callomon, T. M. Dunn, I. M. Mills, *Philos. Trans. R. Soc. London, Ser. A* **1966**, *259*, 499.
41 E. Pantos, A. M. Taleb, T. D. S. Hamilton, I. H. Munro, *Mol. Phys.* **1974**, *28*, 1139.